自然災害科学 *J. JSNDS 15-2 151-174 (1996)*

ARTICLE

Flooding in Sandwip Island in the 1991 Storm Surge Disasters

Hajime NAKAGAWA* • Yoshiaki KAWATA*
• Kazuya INOUE* • Tomonobu TANINO**

Abstract

In this paper, firstly, the numerical simulation model for the simultaneous analysis of storm surges and their flooding in Sandwip island is presented. A model of a cyclone is introduced to obtain the wind fields and the atmospheric pressure which are used for the calculation of the storm surge heights of the 1991 cyclone. Secondly, the combined simulation method of storm surge flooding and the action of residents in the island is presented. A method to simulate the movements of groups of residents during evacuation in response to the storm surge flooding occurring after the coastal dikes have been breached is described. This model is applied to Sandwip island to assess the evacuation systems there. Thirdly, the "designed cyclone" is defined as the cyclone taking the path which generates the maximum volume of flood water carried to Sandwip island. Finally, the countermeasures needed are proposed.

Key words : Storm surge, Cyclone, Flooding, Evacuation system, Bangladesh, Sandwip Island

1. Introduction

The cyclones that strike Bangladesh are generated in the southern area of the Bay of Bengal and in the Andaman Sea. The number of cyclones that annually hit Bangladesh ranges from three to five, and they strike during the pre- and post-monsoon seasons. River floodings also occur in the monsoon seasons. In Bangladesh, the sequential occurrence of such natural disasters caused by cyclones as strong wind, storm surges, and river flooding is frequent.

As Bangladesh is prone to storm surges because of meteorological and topographical conditions, many storm surges and their resultant damages have been recorded. During 32 years from 1960 to 1991, 37 major cyclones have lashed Bangladesh and on the average one major cyclone strikes Bangladesh per year (Choudhury, 1991). As the elevation at high tide ranges from 1 to 3 m, storm surges heights above the astronomical tide are estimated in most cases to be 1 to 4 m and sometimes more

* Disaster Prevention Research Institute, Kyoto University
** Undergraduate Student, Department of Civil Engineering, Faculty of Engineering, Kyoto University

Discussion open until Feburuary 28, 1997

than 7 m. These values are much larger than those for Japan where the recorded maximum storm surge anomaly in Nagoya Harbor of Ise Bay in 1959 was 3.4 m. Choudhury showed that the maximum wind speed was 62.5 m/s, the storm surge height was 6.1～7.6 m, and the number of deaths was 138,000 in the April 1991 cyclone and 61.9 m/s, 6.1～9.1 m, and 500,000, respectively in the November 1970 cyclone.

Flather (1994) simulated the storm surges caused by the both cyclones, using the new formulation which combines the solution of 1D and 2D equations within the same computational framework, differentiated only by factors defining channel width in the delta and wetted surface area. Further, by allowing for inundation using the simple algorithm, this model is possible to simulate the transformation of 1D flow along a river channel into 2D flow as the surface elevation rises above bank level and floods adjacent land area. But it is not clear wheter this model is varid or not because the calculated results of the flooding extent and the water levels on the land are not compared with the actual data.

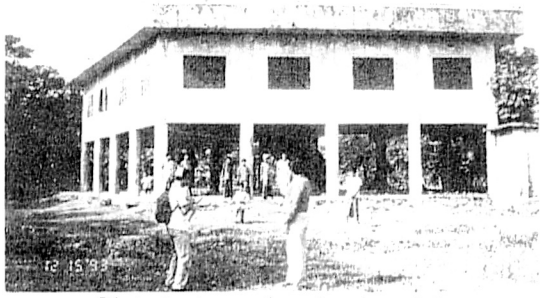

Photo 1 Arrow-shaped cyclone shelter.

In Sandwip island, more than 13,000 people were killed by the storm surge flooding due to the 1991 cyclone. To reduce the number of deaths by cyclones in Bangladesh, evacuation to the cyclone shelter is very effective. **Photo 1** shows an example of cyclone shelters which is very popular arrow-shaped one. Recently, multipurpose cyclone shelters, which are usually used as schools or community centers, have been constructed. In this paper, the methodology to assess the evacuation systems on the basis of the analysis of the storm surge floodings is presented.

2. Numerical Simulation Model of Storm Surges and Resulting Floods

2.1 Basic Equations of Storm Surges and Resulting Floods

The basic equations used to calculate both the storm surges and inundation process on a protected low-lying area are depth-averaged horizontal two-dimensional momentum and continuity equations:

$$\frac{\partial M}{\partial t}+\frac{\partial (uM)}{\partial x}+\frac{\partial (vM)}{\partial y}=fN-gh\frac{\partial (h+z_b)}{\partial x}-\frac{h}{\rho}\frac{\partial p}{\partial x}+\frac{\tau_{sx}}{\rho}-\frac{\tau_{bx}}{\rho} \tag{1}$$

$$\frac{\partial N}{\partial t}+\frac{\partial (uN)}{\partial x}+\frac{\partial (vN)}{\partial y}=-fM-gh\frac{\partial (h+z_b)}{\partial y}-\frac{h}{\rho}\frac{\partial p}{\partial y}+\frac{\tau_{sy}}{\rho}-\frac{\tau_{by}}{\rho} \tag{2}$$

$$\frac{\partial h}{\partial t}+\frac{\partial M}{\partial x}+\frac{\partial N}{\partial y}=0 \tag{3}$$

where M and N are the water discharge per unit width for x (eastward) and y (northward), i.e., as $M=uh$ and $N=vh$ (hereafter called the "flux"), u and v being the respective depth-averaged velocity components of the x and y directions; h the total water depth; z_b the elevation of the bed; p the atmospheric pressure; ρ the density of sea water; f the Coriolis parameter; g the gravitational force per unit mass; τ_{bx} and τ_{by} the respective shear stresses on the bed in the x and y directions; and τ_{sx} and τ_{sy} the shear stresses at the water surface in the x and y directions. Shear stress at the water surface is evaluated as

$$\tau_{sx}=\rho_a f_s W_x\sqrt{W_x^2+W_y^2},\quad \tau_{sy}=\rho_a f_s W_y\sqrt{W_x^2+W_y^2}, \tag{4}$$

where ρ_a is the density of air; f_s the drag coefficient at the water surface; and W_x and W_y the respective wind velocity components of the x and y directions at the surface. Bottom shear stress is assumed to take the relations

$$\tau_{bx}=\frac{\rho g n^2 u\sqrt{u^2+v^2}}{h^{1/3}}-k\tau_{sx},\quad \tau_{by}=\frac{\rho g n^2 v\sqrt{u^2+v^2}}{h^{1/3}}-k\tau_{sy}, \tag{5}$$

where n is Manning's roughness coefficient; and k a constant with the value of 0.25.

These equations are used to calculate storm surges and the resulting floods. In the calculation of the storm surges in the large domain, which is described later, the boundary condition at the coastal lines is that the discharge fluxes M and N normal to the boundary is zero. In the small domain (Sandwip Island) the calculation of inundation is carried out. In this domain, when there are no coastal embankments at the boundaries between the sea zones and land, flood discharge fluxes M and N can be calculated by using the same equations of (1)~(5). At that time, the flood front of the flow is a moving boundary and presents a difficult problem even for computer-aided analysis. The present analysis sacrifices strictness of momentum conservation to some extent to get rid of the complexity at the forefront. The alternative simplified treatment is that if the computation yields a flow depth less than a certain small threshold value, h_{th}, taken as 1 mm, in a mesh, the forefront is regarded as not having arrived yet, so that no outflow flux is generated from this mesh, while inflow flux into this mesh is allowed.

When there are coastal embankments in the small domain, the overflow discharge over the embankments is evaluated, for example, by the formulae (Committee on Hydraulics, JSCE, 1985)

$$\left.\begin{aligned} M\ (\text{or } N) &= \mu h_1\sqrt{2gh_1} && (h_2/h_1\le 2/3)\\ M\ (\text{or } N) &= \mu' h_2\sqrt{2g(h_1-h_2)} && (h_2/h_1> 2/3)\end{aligned}\right\} \tag{6}$$

where μ and μ' are discharge coefficients with the respective values of 0.91 and 0.35; $h_1=H_r-H_0$; $h_2=H_f-H_0$; H_r is the water level on the seaward side; H_0 the elevation of the coastal embankment crown; and H_f the water level on the landward side. In the calculation, h_1 and h_2 are defined at the cells adjacent to the coastal embankments. Overflow occurs when $h_1>0$ and $h_1>h_2$ or $h_2>0$ and $h_2>h_1$. In the case that $h_1>0$ and $h_1>h_2$, the type of overflow is said to be "complete overflow" when $h_2/h_1\le 2/3$, while "submerged overflow" when $h_2/h_1>2/3$ (see Eq. (6)). When $h_2>0$ and $h_2>h_1$, flow fluxes in an opposite direction can be evaluated by Eq. (6) replacing h_1 with h_2. M and N likewise can be evaluated for river dikes. It should be noted that the storm surges and the resulting floods are calclated simultaneously, not separately.

2.2 Cyclone Model

It is necessary first to deal with the cyclone, the main external force and the decider of the wind field in storm surge calculations. A number of cyclone models exist. The Fujii & Mitsuta model (Fujii and Mitsuta, 1986) was adopted for this study as Yamashita got good reproducibility of the storm surges by the 1991 cyclone (Katsura *et al.*, 1992). In this model, the atmospheric pressure field is described by Schloemer's formula as

$$p=p_c+\Delta p\exp\left(-\frac{r_m}{r}\right), \tag{7}$$

where r is the distance from the center of the cyclone; p the pressure at the radial distance r; p_c the central pressure; Δp the difference between the ambient and central pressures; and r_m the radius of the maximum wind speed.

The gradient wind speed, U_{gr}, is obtained by solving the equation of motion

$$\frac{U_{gr}^2}{r_t} + fU_{gr} = \frac{1}{\rho_a}\frac{\partial p}{\partial r} , \tag{8}$$

where r_t, the radius of curvature of the trajectory of the air particle, is evaluated by Blaton's formula as

$$\frac{1}{r_t} = \frac{1}{r}\left(1 + \frac{C}{U_{gr}}\sin\alpha\right), \tag{9}$$

where C is the speed of the cyclone; and α the direction angle of the radius vector measured counterclockwise to the direction of movement. From Eqs. (7), (8) and (9), the gradient wind speed, U_{gr}, is

$$U_{gr} = \frac{1}{2}\left\{-(C\sin\alpha + rf) + \sqrt{(C\sin\alpha + rf)^2 + \frac{4\Delta p r_m}{\rho_a r}\exp\left(-\frac{r_m}{r}\right)}\right\} \tag{10}$$

The wind speed on the ground surface, U_s, can be greater than the friction-free wind, U_{gr}, a little inside along the radius of the maximum cyclonic wind speed. Mitsuta *et al.* confirmed this super-gradient wind effect by analyzing recorded data for typhoons 7705 and 7709 that struck the Nansei Islands (Mitsuta *et al.*, 1978, Yamamoto *et al.*, 1978). Fujii and Mitsuta (1986) formulated this effect as

$$\frac{U_s}{U_{gr}} = G(\xi) = G(\infty) + \left\{G(\xi_p) - G(\infty)\right\}\left(\frac{\xi}{\xi_p}\right)^{e-1}\exp\left[\left(1-\frac{1}{e}\right)\left\{1-\left(\frac{\xi}{\xi_p}\right)^e\right\}\right] \tag{11}$$

where $\xi = r/r_m$. The parameters $e = 2.5$, $\xi_p = 0.5$ and $G(\xi_p) = 1.2$ are determined from these data. The function $G(\xi)$ increases with the increase of ξ reaching the maximum value $G(\xi_p)$ at $\xi = \xi_p$. Thereafter, it decreases with further increases of ξ and approaches $G(\infty)$ asymptotically at $\xi \to \infty$. The deflection angle of the surface wind to the isobars is assumed to be 30°. Consequently, the components of the wind speed at the position of (x, y) in the storm surge calculations, W_x and W_y are

$$W_x = -\frac{(x-x_c) + \sqrt{3}(y-y_c)}{2r}U_s \quad , \quad W_y = \frac{\sqrt{3}(x-x_c) - (y-y_c)}{2r}U_s \tag{12}$$

where (x_c, y_c) is the cyclone's position and $r^2 = (x-x_c)^2 + (y-y_c)^2$.

2.3 Finite Difference Equations

The system of equations is integrated numerically. The values to be calculated are the total water depth h and the "flux", M and N. Fluxes M, N and the velocities u, v are defined in the middle of and normal to each cell face. The total water depth h is defined in the center of each cell. Therefore, there are two staggered meshes associated with the respective "flux" (or velocity) components. Leap-frog scheme using an upwind finite-difference scheme for the convection terms in momentum equations was adopted (Inoue *et al.*, 1993).

3. Combined Simulation Model of Storm Surges Flooding and The Evacuating Action of Residents

The refuge network (main network) is composed of refuges (cyclone shelters), evacuation routes and nodes in the study area (Sandwip Island). The study area from which it is necessary to evacuate people is determined by the numerical simulation of flooding. In this case, all the people in Sandwip island should evacuate to the cyclone shelters because the elevation of the whole island is very low, so that the study area is the whole island. Only roads familiar to the residents, such as the main local roads in the island are designated routes for evacuation.

Whether the cyclone shelters and the evacuation routes are adequate (the number of cyclone shelters, the height of shelters, the number of persons to be accommodated, the elevation of the evacuation routes, the number of evacuation routes, etc.) can be judged from the calculations of water depth and the simulation of evacuation. For example, if the cyclone shelters or evacuation routes are deeply submerged, they would not be suitable and new cyclone shelters or routes would have to be established. This simulation method therefore provides a reasonable ground to establish better evacuation systems.

In this chapter, a simulation model of evacuating action of residents which is linked with a numerical simulation model of storm surges flooding is presented (Takahashi *et al.*, 1990).

3.1 Modeling of Refuge Network

In order to introduce the water depth at each mesh in the calculation as a information whether the cyclone shelters or routes are submerged or not, actual evacuating routes are slightly modified as shown in **Fig.1**. Namely, modified routes are composed of the paths which run through the center of the meshes, and the position of a node (the road intersection or the refuge) is set to the center of a mesh. An evacuating route is divided into elements and each of them corresponds to a certain mesh in the calculation of inundation. For example, in **Fig.2**, mth element in the nth route correspond to the mesh of $(i-3/2, j+1/2)$.

It is very difficult to simulate the action of each person in the case that the calculation area is large and great many people live there because of limitations of the capacity of a computer memory and the

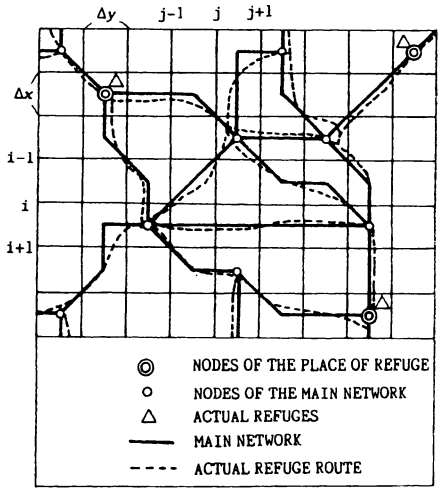

Fig.1 Arrangement of a refuge network.

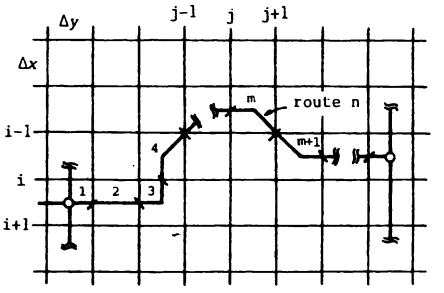

Fig.2 Elements of a refuge route corresponding to cells of the inundation calculation.

executing time of computation. In this paper, the minimum unit of residents is defined as a group of inhabitants who are living in the mesh of a calculation for storm surges flooding. The initial position of this group is divided broadly to two categories. One is on the evacuating networks and the other is out of networks. In the former case, this group can evacuate to the cyclone shalter by directly using the networks. While in the latter case, other paths connected with a node of the networks must be established. Then, the blocks of residential area composed of sub-networks are introduced as shown in **Fig.3**. An evacuating group in this area at first goes to the nearest node of main networks by using the shortest way in the block, then it evacuates to the nearest cyclone shelter on the main networks. In the block of a residential area, the imaginary nodes are set up in the center of each mesh and the imaginary routes are also installed between each node.

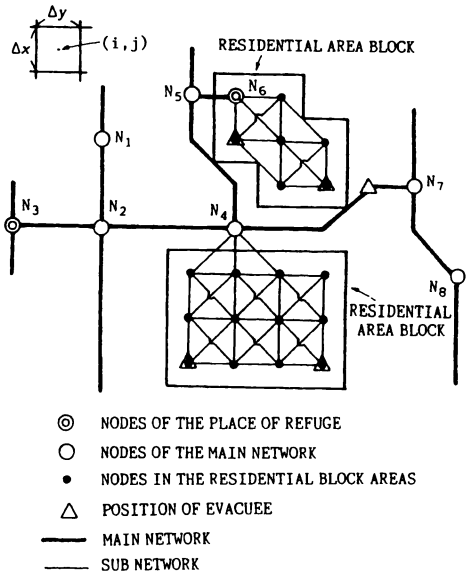

Fig.3 Relation between the refuge network and the position of residents in a residential block area.

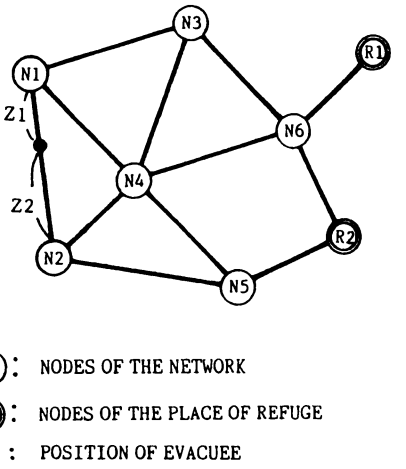

Fig.4 Relation between the refuge network and the position of an evacuee.

3.2 Modeling of Actions of Residents

Generally, it can be considered that the distance between a location of residents and that of a cyclone shelter is one of the most important factors when the residents select a certain cyclone shelter among others. From this point of view, it is assumed that the way of selection of the optimal cyclone shelter can be formulated as a selection problem of the shortest-path algorithms in network theories. **Figure 4** shows the relationship between refuge networks and position of a group of resident on a route of them. In this figure, the group is located at the distance, $Z1$, from the node of **N1** and the distance, $Z2$, from the node of **N2**. The evacuating action is simulated as follows:

(a) The shortest distance both from the node, **N1**, and the node, **N2**, to an arbitrary refuge node is calculated by

$$(F_{ij})_{min} = \min \{F_{N1,1}+Z1, \cdots \cdots, F_{N1,\ell}+Z1, F_{N2,1}+Z2, \cdots \cdots, F_{N2,\ell}+Z2 \quad (13)$$

where F_{ij} is the shortest distance between an intersection node, **Ni**, and a refuge node, **Nj**, and this is

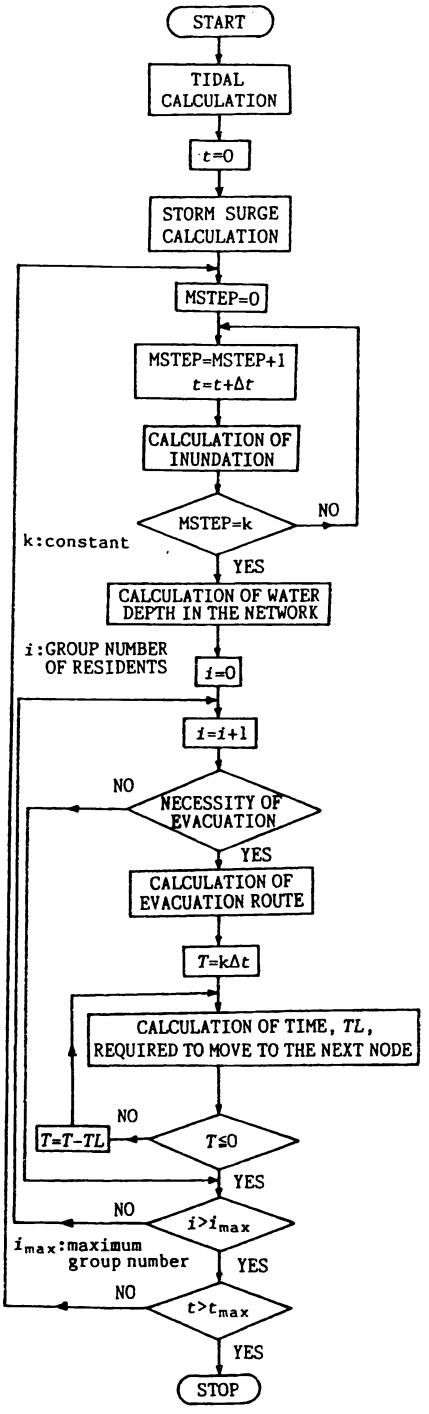

Fig.5 Flow chart for the method of simulating evacuation linked with an inundation calculation.

solved by using Warshall-Floyd method (Iri *et al.*, 1976); and ℓ the total number of refuges.

(b) If it is assumed that the solution of Eq. (13) is $F_{N1,R1}+Z1$, i.e., the shortest path is the approach route to the refuge node, **R1**, through intersection node, **N1**, the time, TL, required from a position of the group to the node, **N1**, is calculated by using the walking speed of the evacuating group. The details of walking speed will be described later.

(c) Let T be the time interval of calculation of evacuating action, and if $TL > T$, i.e., an evacuating group can not arrive at the node **N1** within the time T, a new position between the last position and **N1** is calculated by using the value T and walking velocity. While if $TL < T$, an evacuating group can reach the node **N1** and still remains the time which can be used for further motion. If **N1** is a refuge place, evacuating action of this group finishes. But if not, $T-TL$ is replaced by new T and going back to (a), then, remaining time is consumed to proceed through **N1**.

The same procedure mentioned above is repeated and it is possible to simulate the evacuating action of residents. The flow-chart of the simulation method of evacuation linked with an inundation analysis is shown in **Fig.5**.

When a part of networks is covered with water, a walking speed on it becomes slow corresponding to the water depth. In this paper, the actual length of the route is apparently lengthened in order to consider the effect of water depth to a walking speed. This apparent length of a route is defined as follows (Nishihara, 1983):

$$d^t_{(i,j)} = (1/W^t_{(i,j)})\, d_{(i,j)} \ , \quad \text{(unit : m)} \tag{14}$$

$$W^t_{(i,j)} = 1 - h^t_{(i,j)}/h_c \ , \quad (W^t_{(i,j)} > 0) \ , \quad \text{(unit : m)} \tag{15}$$

where $h^t_{(i,j)}$ is the water depth of the mesh of (i,j) at time $= t$; $d_{(i,j)}$-the actual length of the route in the mesh of (i,j); $d^t_{(i,j)}$ the apparent length of the route in the mesh of (i,j) at time $= t$; and h_c the critical water depth in which an adult can not move safely, and it is assumed that it takes the

value 0.7 m with reference to the example that an adult could have a narrow escape at the depth of 70 cm in water during the Ise-Bay typhoon (Institute for Fire Safety and Disaster Preparedness, 1987). Therefore, it is defined that if the water depth at a certain mesh is more than 70 cm, the length of the route in this mesh is set to infinity and no one can move there even if the water depth decreases later.

Walking speed in the evacuating action is affected by several factors, i.e., environmental factors such as the season, weather, time, brightness, etc., physical factors such as sex, age, health, fatigue, etc., collateral factors such as clothes, baggages, etc., psychological factors such as a sensation of fear, well known place or not, etc. and the factors of assembly such as number of people in a group, density of people on a road, etc.. It is very difficult to estimate the walking speed in the midst of evacuation correctly because these factors are connected with each other. Here, in the same way as Nishihara (1983) did, retardation of walking speed due to congestion and fatigue is taken into consideration. The walking speed is defined as follows:

$$V_n^{t'} = T^{t'} U_n^{t'} \tag{16}$$

$$T^{t'} = 1.0/\{0.982+\exp(1.12t'-4.0)\} \ , \ \text{(unit : hour)} \tag{17}$$

$$U_n^{t'} = U_0 - 0.241\rho_n^{t'} \ , \quad (\rho_n^{t'} < 3.85) \tag{18}$$

$$U_n^{t'} = 0.49 \ , \quad (\rho_n^{t'} \geq 3.85) \tag{19}$$

where $V_n^{t'}$ is the walking speed of a group on the nth route at time $= t'$; $T^{t'}$ the reduction rate of walking speed due to fatigue according to the time required since commencement of evacuation; t' the time required since action of evacuation is commenced; $U_n^{t'}$ the walking speed of a group on the nth route at time $= t'$, which is depend on the density of people on the route but independent of fatigue; U_0 the initial walking speed; $\rho_n^{t'}$ the density of people in a group on the nth route at time $= t'$, and it is written as follows:

$$\rho_n^{t'} = M_n^{t'}/(B_n L_n) \ , \ \text{(unit: person/m}^2\text{)} \tag{20}$$

in which $M_n^{t'}$ is the total number of residents on the nth route at time $= t'$; B_n the width of the nth route (unit: m); and L_n the actual length of the nth route (unit: m).

4. Storm Surges and Resulting Floods in Sandwip Island by the 1991 Cyclone

4.1 Computational Domain

There are two computational domains: One is a large scale domain which covers all the coastal areas of Bangladesh (hereafter called the "large domain"). The other is a small scale domain which covers the whole Sandwip island (hereafter called the "small domain").

(1) Large Domain

Figure 6 shows the large domain with the grid size $\Delta x_L = 1767$ m for longitude and $\Delta y_L = 1894$ m for latitude. The number of cells for longitude is 194 and for latitude, 117. Data on sea bed elevation are obtained from bathymetric charts with the scale 1:300,000. Though the deep sea zones with more than 800 m exist in the south-west side of this domain, the eastern part of the sea is very shallow, the depth being less than about 20 m until 200 km off-shore from Sandwip island. The tidal range of most of the ports in Bangladesh is about 4~6 m due to such geomorphological conditions. Moreover, when a cyclone approaches this region, sea level becomes large due to the shallow water effects.

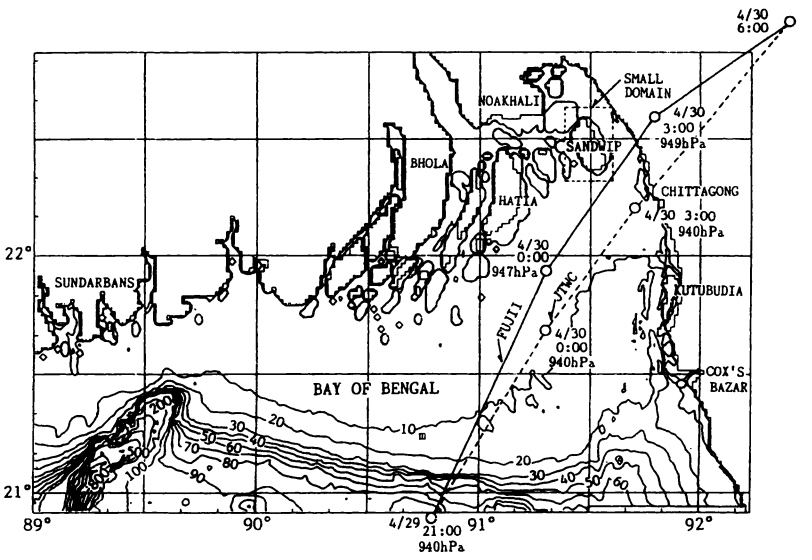

Fig.6 Large scale computational domain.

(2) Small Domain

The area of the island is about 220 km^2. **Figure 7** shows the small domain with the grid size $\Delta x_S =$ 441.75 m for longitude and $\Delta y_S = 473.50$ m for latitude. The number of cells for longitude is 52 and for latitude 76.

The small domain is also shown in **Fig.6** enclosed with dashed lines rectangularly. As topographical maps of Sandwip island are not available, precise ground elevation in the island is unknown. This island is very flat with mean elevation of about 2.0 m from mean sea level with neither mountains nor uplands. This island was formed by the deposition of the sand transported by the Brahmaptra and Ganges rivers. At the present time, the course of the river is changing due to fluvial channel process and the river mouth now exists near the Bhola and Hatia islands. Consequently, the north part of Sandwip island has a tendency to be eroded, partly with deposition in the south. This means the island is moving southward.

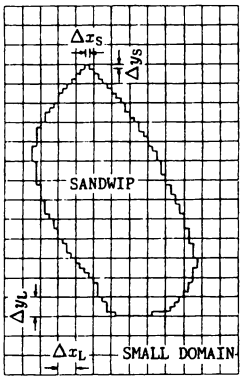

Fig.7 Small scale computational domain.

4.2 Conditions of Calculation

(1) Tracking Paths of the 1991 Cyclone

The tracking paths and the pressure data of the 1991 cyclone were gathered and presented by JTWC (U.S. Army and Air Force Joint Typhoon Warning Center), BRC (Bangladesh Red Crescent), and SPARRSO (Space Research and Remote Sensing Organization) respectively. Fujii (Katsura *et al.*, 1992) carried out an objective pressure analysis for the 1991 cyclone on the basis of the JTWC data and the 3 − hourly observed data at 18 stations in Bangladesh. He modified the JTWC data (dashed lines) as shown in **Fig.6.** In this study, Fujii's modified data (solid lines) are used because his data are more faithful to the observed data.

(2) Tidal Conditions

It is usual that the astronomical tide level, which is estimated by using the constituents obtained at the nearest tide station, be given at the open boundary. However, in Bangladesh, as the number of tide stations is few and the open boundary is wide as seen in **Fig.6**, charts of the tidal components of M_2, S_2, K_1, O_1, N_2, Q_1, and M_f predicted by Schwiderski (1979, 1981a, 1981b, 1981c, 1981d, 1981e, 1982) were used to specify the open boundary condition of the tide. In these charts, the tide amplitude, ϕ, and the tide Greenwich phase, δ, are tabulated from 0.5° at an interval of 1° in each direction of both longitude and latitude. The tide, ζ, for each tidal component is calculated by

$$\zeta = \phi \cos(\sigma t + \chi - \delta), \tag{21}$$

where σ is the tide frequency ($= 1.40519\times10^{-4}$ sec^{-1} for M_2; $= 0.72921\times10^{-4}$ sec^{-1} for K_1; $= 1.37880\times10^{-4}$ sec^{-1} for N_2; $= 1.45444\times10^{-4}$ sec^{-1} for S_2; $= 0.67598\times10^{-4}$ sec^{-1} for O_1; $= 0.64959\times10^{-4}$ sec^{-1} for Q_1; $= 0.53234\times10^{-5}$ sec^{-1} for M_f.)

$\chi = 2\pi(h_0 - s_0)/180$rad for M_2; $\chi = \pi(h_0+90)/180$rad for K_1; $\chi = 2\pi(2h_0 - 3s_0 + p_0)/180$rad for N_2; $\chi = 0.0$rad for S_2; $\chi = \pi(h_0 - 2s_0 - 90)/180$rad for O_1; $\chi = \pi(h_0 - 3s_0 + p_0 - 90)/180$rad for Q_1; $\chi = 2\pi s_0/180$rad for M_f.

$h_0 = 279.69668 + 36000.768930465T + 3.03\times10^{-4}T^2$.

$p_0 = 334.329653 + 4069.0340329575T - 0.010325T^2 - 1.2\times10^{-5}T^3$.

$s_0 = 270.434358 + 481267.88314137T - 0.001133T^2 + 1.9\times10^{-6}T^3$.

$T = (27392.500528 + 1.0000000356DD)/36525$.

$DD = D + 365(Y-1975) + [(Y-1973)/4]$.

Y is the year ($\geqq 1975$); D the day ($D = 1$: January 1st); t the universal standard time (sec); ϕ and δ are respectively Schwiderski's tide amplitude (m) and tide Greenwich phase (rad); and [ ] is the integer part.

(3) Boundary Conditions

Large Domain The tide, ζ, at open boundaries was estimated by using Eq. (21). As both amplitude, ϕ and phase, δ in Eq. (21) are given only from 0.5° at an interval of 1.0° in both longitude and latitude, we used interpolation or extrapolation to estimate ϕ and δ at each mesh on open boundaries as follows: As there are only 10 positions where ϕ and δ are given around the large domain (88.5°, 20.5°), (88.5°, 21.5°), (89.5°, 20.5°), (89.5°, 21.5°), (90.5°, 20.5°), (90.5°, 21.5°), (91.5°, 20.5°), (91.5°, 21.5°), (91.5°, 22.5°), and (92.5°, 20.5°), ϕ and δ at each mesh on open boundaries were interpolated or extrapolated by using the above data. After that, tide ζ at each mesh on open boundaries was estimated by using Eq. (21).

Moreover, the cyclone effects, consisting of the water surface being lifted by the drop in atmospheric pressure, and wind drift were considered at open boundaries, and were respectively

$$\Delta h_p \text{ (cm unit)} = 0.991(p_\infty - p) \quad \text{(hPa unit)} \tag{22}$$

$$\Delta h_w = \beta \Delta h_p \tag{23}$$

where Δh_p is the incremental elevation in the water level caused by the drop in pressure; Δh_w the incremental elevation in the water level caused by wind drift; p_∞ the ambient atmospheric pressure, taken as 1010hPa; and β the numerical constant, taken as 1.0 (Nakatsuji *et al.*, 1993).

The conditions of fluxes at open boundaries are $\partial M/\partial x = 0$, $\partial M/\partial y = 0$, $\partial N/\partial x = 0$, $\partial N/\partial y = 0$. At land side boundaries, the components of the fluxes perpendicular to the land are all zero, i.e. no floodings occur.

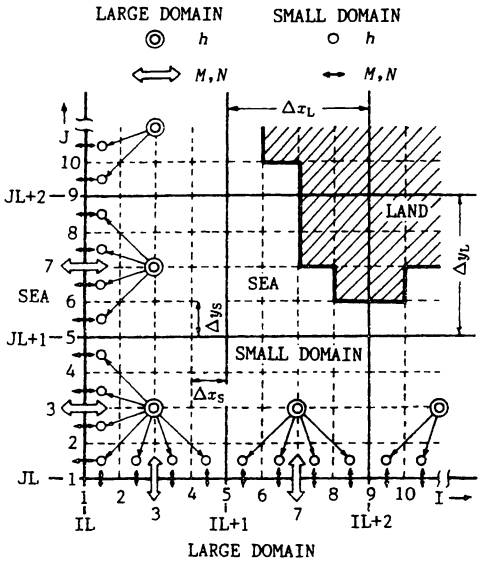

Fig.8 Conditions to connect the large and small domains.

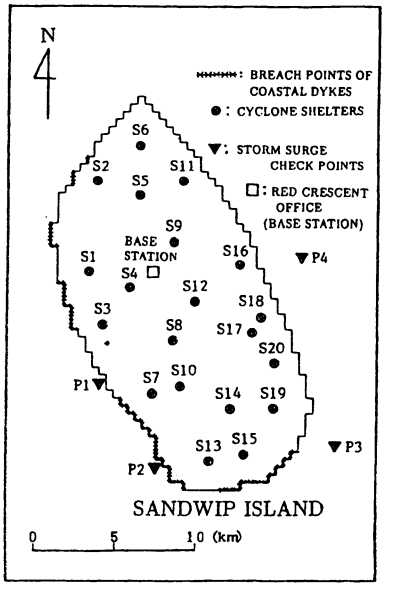

Fig.9 Points of the coastal dikes breached by the storm surges in 1991 cyclone.

Small Domain In the small domain enclosed by the broken lines rectangularly shown in **Fig.6**, calculated results at the lines in the large domain are stored in new data sets and used as boundary conditions in the small domain for the simultaneous calculation of storm surges and their-induced flooding. The connection conditions between the large domain and the small one are that the same hydraulic values as calculated in a mesh in the large domain were given to 4 meshes in the small domain as shown in **Fig.8**. Coastal dikes with a height of about 2 m from a ground level had been constructed before the 1991 cyclone, but the dikes with the symbol × and thick lines shown in **Fig.9** were destroyed by the storm surges in that cyclone. The dikes with a height of 2 m from a ground level are arranged along the coastal meshes in the calculation and the breaches of the coastal dikes are supposed to occur at the positions shown in **Fig.9**, while heights of the dikes are supposed to become the same as ground levels instantaneously when the tide level becomes higher than the height of an arbitrary dike.

(4) Initial Conditions

The initial sea water levels in the large and the small domains are given by using the relation between chart datum level (C.D.L.) and mean water level (M.S.L.), i.e. M.S.L. is 2.1 m higher than C.D.L. (Katsura *et al.*, 1992).

The tidal calculation without the cyclone effects was executed for 3 days before the attack of the cyclone, followed by the calculation of the storm surges considering the effects of the cyclone, i.e. the tidal calculation was done for 3 days from 25 April, 1991 (D = 31 (Jan.) + 28 (Feb.) + 31 (Mar.) + 25 (Apr.) = 115) to 27 April, 1991 and then the storm surge calculation was done for 66 hours from 0:00 on 28 April, 1991 to 18:00 on 30 April, 1991. These times are Greenwich time, and local time in Bangladesh is 6 hours earlier than Greenwich time. As a result, the storm surge calculation was carried out from 6:00 on 28 April to 0:00 on 1 May in local time. Hereafter, time is expressed in local time.

The following values are used in the calculations: $f = 5.33 \times 10^{-5}$ (rad/sec), which is evaluated at 21.5° North Latitude; ρ = 1030 (kg/m^3); ρ_a = 1.293 (g/m^3); f_s = 0.0026 (Katsura *et al.*, 1992), k =

0.25, r_m = 60 (km) (Katsura *et al.*, 1992). For Manning's roughness coefficient, n = 0.02 was used for the sea bed and n = 0.067 for the land bed in Sandwip island (Inoue *et al.*). Time step, Δt_L, was 20 seconds for the large domain and Δt_S was 5 seconds for the small one. The inflow discharges from rivers into the large domain were not considered in the calculations.

4.3 Calculated Results and Discussion

(1) Storm Surges in the Large Domain

Figures 10, 11, and **12** show respective wind vectors, wind field calculated from Fujii & Mitsuta's cyclone model, and surge heights. These figures are nearly the same as Yamashita's results (Katsura *et al.*, 1992), except that the open boundary conditions are slightly different from ours and a little difference can be seen about surge heights. **Figure 13** shows the temporal changes in the tide level at

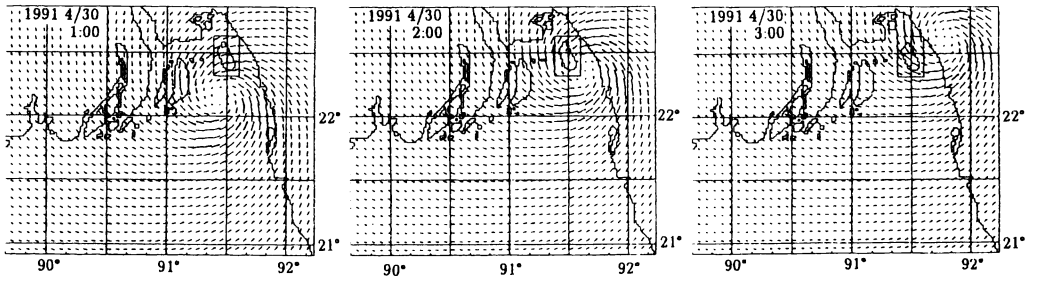

Fig.10 Wind vectors calculated from Fujii & Mitsuta's cyclone model.

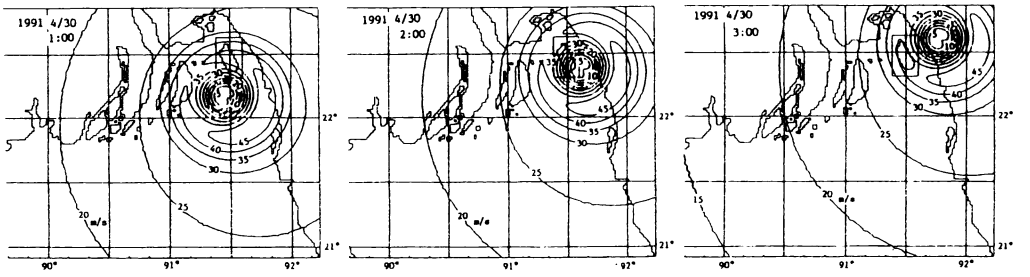

Fig.11 Wind field calculated from Fujii & Mitsuta's cyclone model.

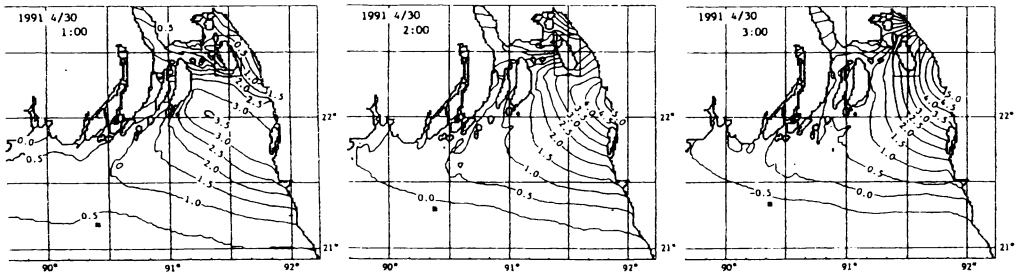

Fig.12 Calculated surge heights.

Chittagong, Cox's Bazar, and Sandwip (source of the observed data is Katsura *et al.*, 1992). The positions of four points, P1～P4, of Sandwip are shown in **Fig.9**. The observed data in Chittagong and Cox's Bazar are fairly well explained by the calculations, so that the storm surges in the large domain seem to be well reproduced by the calculations.

(2) Storm Surge Floodings in Sandwip Island

Figure 14 shows calculated flooded areas in Sandwip island under the conditions that parts of the coastal dikes as shown in **Fig.9** were destroyed (flooding by the overflow and dike breaches occurred). The closed circles in these figures indicate positions of the cyclone shelters. As the peak of the water level higher than 4 m (height of the dike crown is 4 m from M.S.L.) occurred at about 2:30 on 30 April at P1 point which is situated south-west side of the island and at about 3:30 at P4 point on the south-east side (**Fig.13**), inundation due to the overflow from the coastal dikes on the south-west side at first occurred at about 3:00. Flooding from the north-east side happened at about 4:00, with strong flooding from north side, as well. From these calculated results, the coastal dikes along the south-west of the island would most likely be first destroyed by the storm surges, followed by strong floodings from the north and east sides of the island. This prediction is supported by the facts obtained from our field surveys.

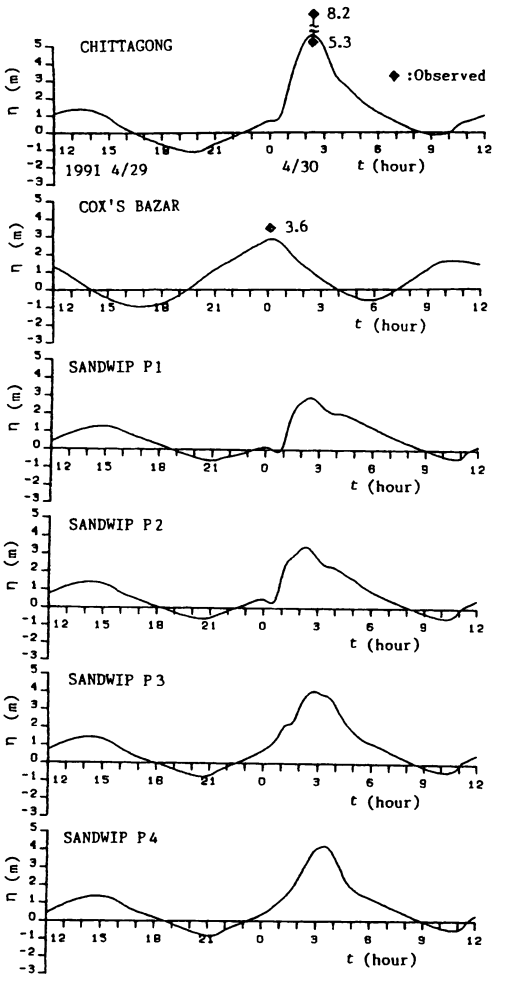

Fig.13 Temporal changes in the tidal level.

Figure 15 shows the calculated temporal changes in the water depth at each cyclone shelter in the case of the breach of the coastal dikes. Symbols, S5, S8 etc. in this figure are the positions of the cyclone shelters shown in **Fig.9**. The northern part of the island had been flooded about 3.5 m deep, while the south and central area was flooded about 2.0 m deep. The data obtained from our field survey included this central and southern parts of the island, so that the storm surge floods in the island are fairly well explained by the calculations. The actual phenomena which occurred in the island on 30 April, 1991 are assumed to have followed the processes of inundation calculated in the case of breaching of the coastal dikes, and 13,090 persons were killed by the storm surges in this island whose population was 264,863 (the number is based on the national census in 1981).

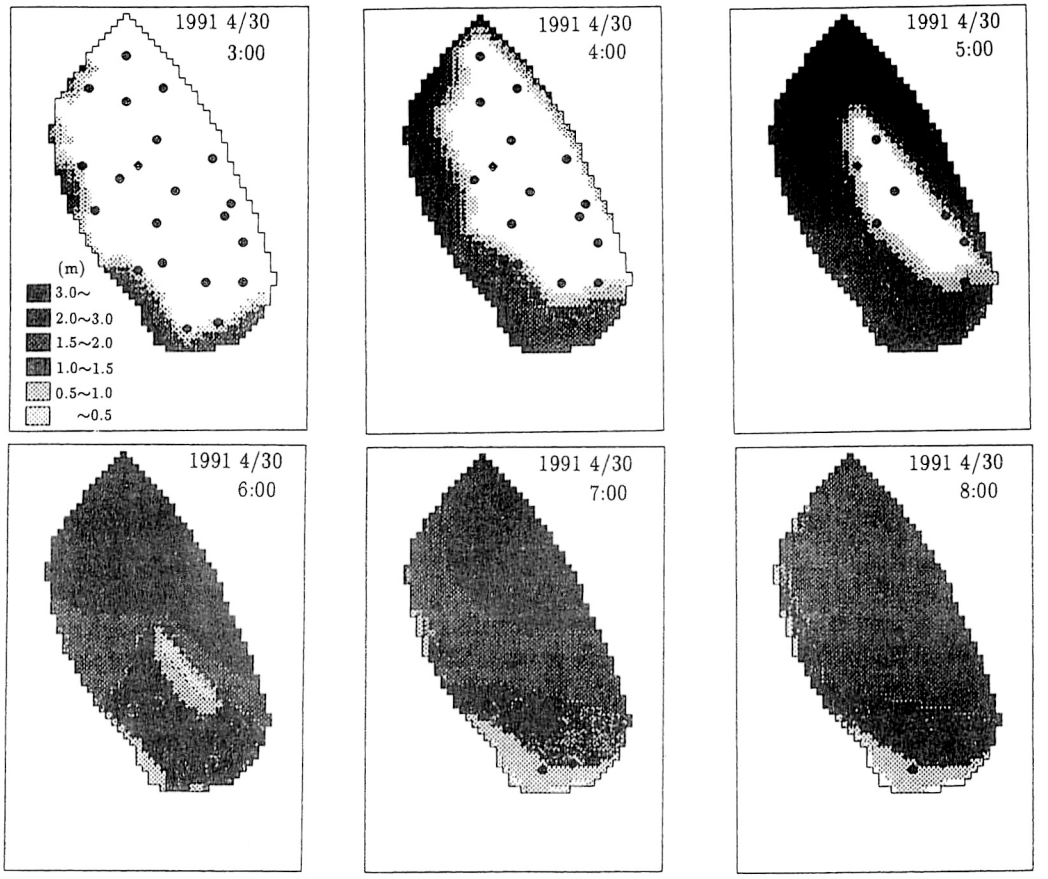

Fig.14 Flooded areas calculated in Sandwip island (breach of dikes).

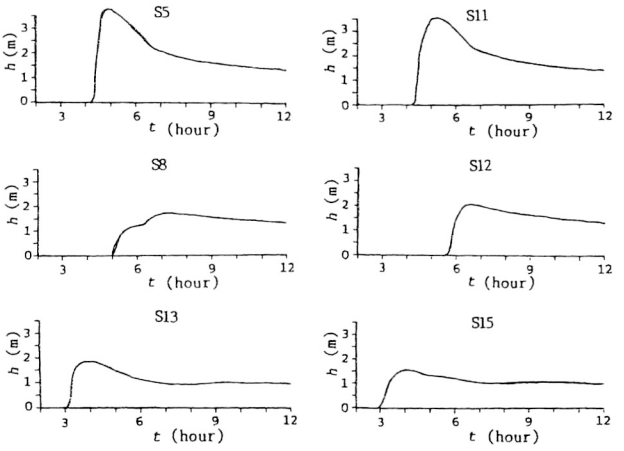

Fig.15 Temporal changes of the water depth at each cyclone shelter in the calculations (breach of dikes).

5. Simulation of the Evacuation of the Residents of Sandwip Island and Its Analysis

5.1 Condition of Calculation

The refuge network used in the calculation is shown in **Fig.16**, and is composed of main roads and intersections, the width of all the roads being assumed to be 5 m. There are 20 cyclone shelters as refuges and the positions were decided based on the field survey and maps obtained from BRC. BRC office was chosen to be the base station from where evacuation orders would be issued. The evacuation order is assumed to spread in concentric circles from the base station with the residents starting to take refuge as soon as they receive the evacuation order. There are 122 intersection nodes including 20 cyclone shelters as refuges. 710 groups of 400 persons each were arranged in 87 residential blocks based on the density of the population in this island. As we could not obtain precise road maps or precise distribution of population in the island, the residential area and network include many uncertainties. Although the calculated results may be unrealistic, the methodology to evaluate the risk against the storm surges under the condition of the evacuation action of the residents is so important, that we present it in this subsection.

The simulation cases are shown in **Table 1**. Two propagation speeds for the evacuation order were introduced: $U_p = 5\,\mathrm{m/sec}$, which corresponds to the order for evacuation being issued by a siren and $U_p = 1.4\,\mathrm{m/sec}$, when a sound truck or a motor

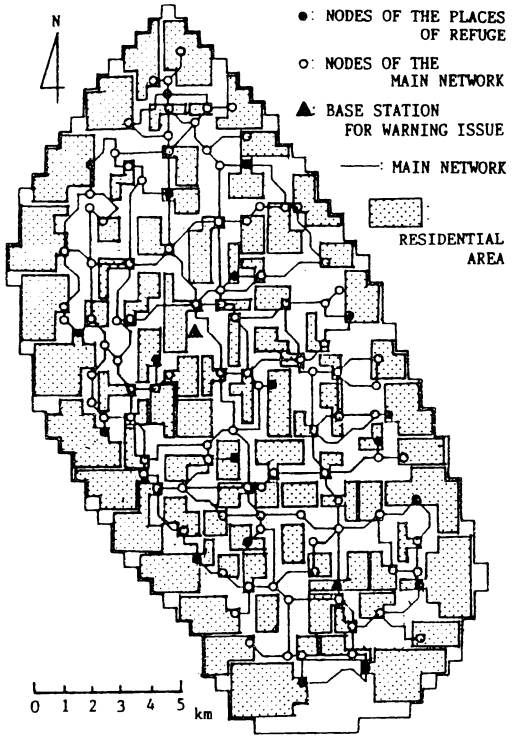

Fig.16 Refuge network in Sandwip island.

Table 1 Simulation cases for the evacuation movements of residents in Sandwip island.

CASE 1-A	The propagation speed of the evacuation order is 1.4 m/sec; not related to flooding.
CASE 1-B	The propagation speed of the evacuation order is 5.0 m/sec; not related to flooding.
CASE 1-C	Simultaneous evacuation; not related to flooding.
CASE 2-A	Residents do not take refuge until they receive the evacuation order when the propagation speed is 1.4 m/sec. The order is issued at the same time as the overflow.
CASE 2-B	Residents do not take refuge until they receive the evacuation order when the propagation speed is 5.0 m/sec. The order is issued at the same time as the overflow.
CASE 2-C	Simultaneous evacuation; related to flooding by the overflow.
CASE 3-A	Residents do not take refuge until they receive the evacuation order when the propagation speed is 1.4 m/sec. The order is issued at the same time as the breaches of the coastal dikes
CASE 3-B	Residents do not take refuge until they receive the evacuation order when the propagation speed is 5.0 m/sec. The order is issued at the same time as the breaches of the coastal dikes.
CASE 3-C	Simultaneous evacuation; related to flooding by the breaches of the coastal dikes.

bicycle is used (Nishihara, 1983). Residents would not take refuge until the evacuation order reaches them. Evacuation orders would be issued at the same time as the dike breach. The initial walking speed U_0 is taken as 1.4 m/sec. CASE 1 has no relation with storm surge floodings. The bank breaches do not occur in CASE 2, while they do in CASE 3.

5.2 Calculated Results and Discussions

(1) Prior Evacuation

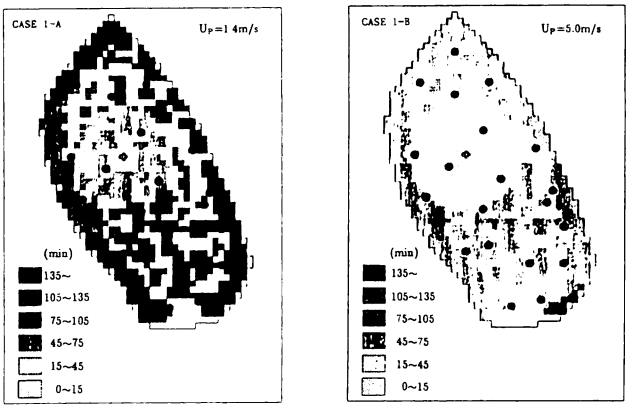

Fig.17 Distribution of the time required for evacuation orders to reach the refuge groups.

It is very important to obtain information about the number of successfully and unsuccessfully evacuated persons, the mean time required for successful and unsuccessful evacuation, and time required to have the evacuation order calculated under the condition of no flooding because the timing of issuing the evacuation order could then be estimated.

The distribution of the time required for the evacuation order to reach the refuge groups is shown in **Fig.17**. The northern and southern parts of the island, which are far from the base station, would need about two and a half hours in CASE 1-A and about 45 minutes in CASE 1-B to get the evacuation order. It is thus understood that in reality, base stations are needed at the northern and southern coastal areas.

The distribution of the time required for evacuation in CASE 1 is shown in **Fig.18**. This figure shows that there are some cells which indicate that it would take more than one hour to arrive at a refuge. As the coastal areas have been proved to be very dangerous during storm surges, new shelters should be built in these places. Consequently, the

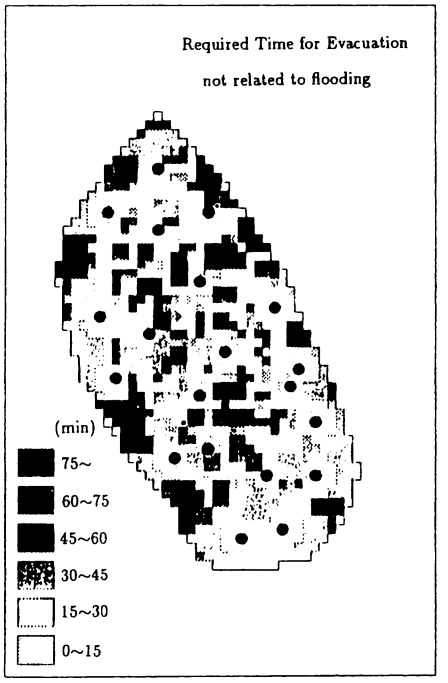

Fig.18 Distribution of the times required for evacuation in CASE 1.

information about where and how many cyclone shelters and base stations are needed can be obtained by this simulation.

(2) Evacuation during Floodings

Figure 19(a) shows the calculated results concerning the state of evacuation for one hour after the dike breach. There would be many groups who would not start to take refuge in CASE 3-A because the evacuation order had not reached them. Some groups would have been caught by flood water around the south-west coastal area. However, groups situated near the base station would successfully evacuate. As the propagation speed of the evacuation order was faster in CASE 3-B than in CASE 3-A, many groups would successfully evacuate except the groups situated in the southern area, where they would not have started to take refuge. **Figure 19(b)** shows the state of evacuation two hours after the dike breach. Many groups would have been caught by flood water in CASE 3-A, while almost all the groups

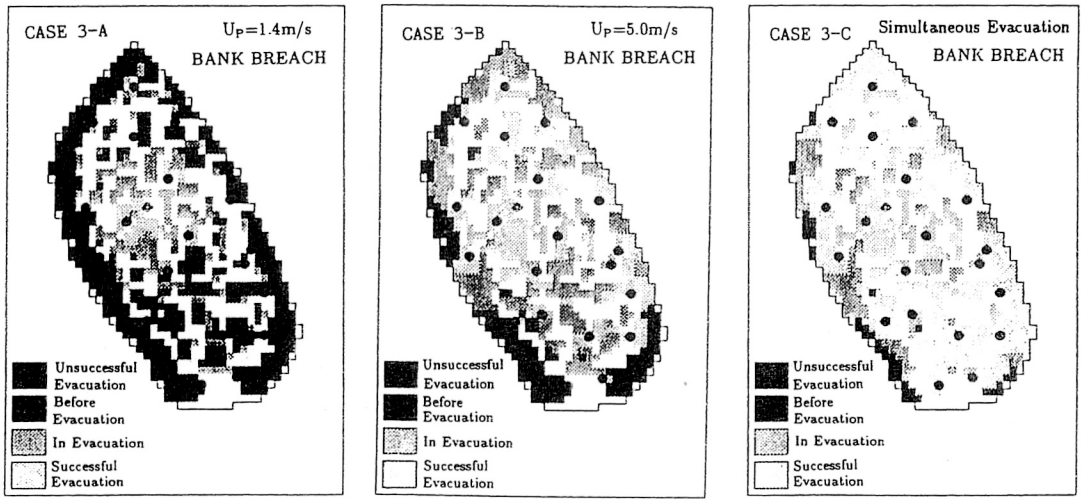

Fig.19(a) State of evacuation at one hour after the dike breach.

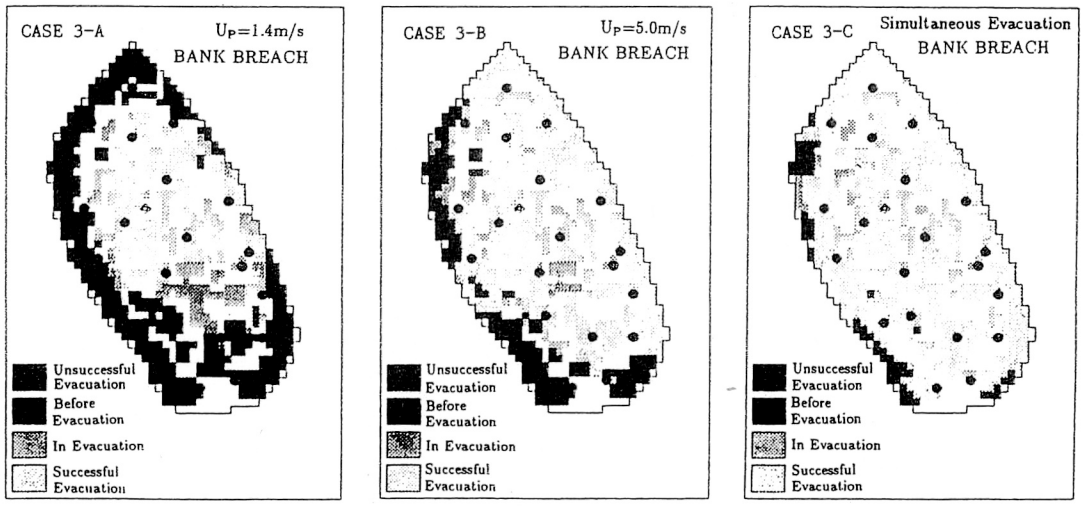

Fig.19(b) State of evacuation at two hours after the dike breach.

Table 2 Calculated results about evacuation movements of residents in Sandwip island.

CASE No.	Number Successfully Evacuated (person)	Number Unsuccessfully Evacuated (person)	Mean Time Required for Successful Evacuation (sec)	Mean Time Required for Unsuccessful Evacuation (sec)
1-A	274,400	9,600	1,728	2,359
1-B	284,000	0	1,749	0
1-C	284,000	0	1,749	0
2-A	171,600	90,000	1,710	419
2-B	271,200	12,800	1,898	2,507
2-C	283,200	800	1,923	5,550
3-A	118,000	164,400	1,825	440
3-B	204,800	79,200	1,931	1,315
3-C	254,800	29,200	1,924	2,217

would have successfully evacuated in CASE 3-C except the groups situated around the south-west coastal area.

Table 2 gives the number of successful evacuees (Number Successfully Evacuated) and of evacuees unable to arrive at a cyclone shelter (Number Unsuccessfully Evacuated), mean traveling time from the start of evacuation to arrival at a shelter (Mean Time Required for Successful Evacuation) and the mean traveling time until unsuccessful evacuees were caught by flood water (Mean Time Required for Unsuccessful Evacuation) 7,000 seconds after the dike breach or the overflow. It would take about 30 minutes for successful evacuation, with that time not being seriously affected by differences in the occurrence of the dike breach, or by propagation speed of the evacuation order. 9,600 persons would be in evacuation in CASE 1-A even at 7,000 seconds after starting to take refuge. There would be more than 160,000 persons unable to arrive at a shelter in CASE 3-A, and about 80,000 unable to arrive at a shelter in CASE 3-B. This means that in reality, sudden dike breaches during severe storm surges cause catastrophic disasters.

It is found from CASEs 2 and 3 that as the propagation speed of the evacuation order increases, the numbers of evacuees unable to arrive at a cyclone shelter decrease, while the mean traveling time until unsuccessful evacuees are caught by flood water becomes larger. While it is easy to understand that fast propagation speed of an evacuation order decreases the numbers of unsuccessful evacuees, it is ostensibly strange that the faster the propagation speed of the evacuation order is, the longer the traveling time of the unsuccessfully evacuated residents becomes. However, the reason for this is that the refugees first move to the nearest cyclone shelter which is not yet inundated in the early stage, but as time proceeds, the route to this nearby shelter becomes inundated gradually, so that the refugees have to move toward a second, more distant shelter. When the refugees would finally be caught by flood water, the traveling time of the unsuccessfully evacuated residents would become longer. Consequently, evacuation orders would have to be issued at least 30 minutes before a dike breach, and the propagation speed of that information would have to be faster than 5 m/sec, for all evacuees to arrive safely at cyclone shelters. In this calculation, there is no restriction about the number of persons to be accommodated. Since the number of cyclone shelters is insufficient to accommodate the 260,000 refugees, this should be taken as a warning that sufficient number of cyclone shelters must be constructed.

6. Risk Assessment Against Designed Cyclone

6.1 Designed Cyclone

The 1991 cyclone being the severest one which hit Bangladesh, we define this cyclone as the "designed scale cyclone" and use its characteristics to "design" a cyclone scale for Sandwip island; this was established as follows: **Figure 20** shows the tracking paths of the "designed scale cyclone". Eight hypothetical tracking paths at an interval of 10 km were set 80 km westward from the actual path of

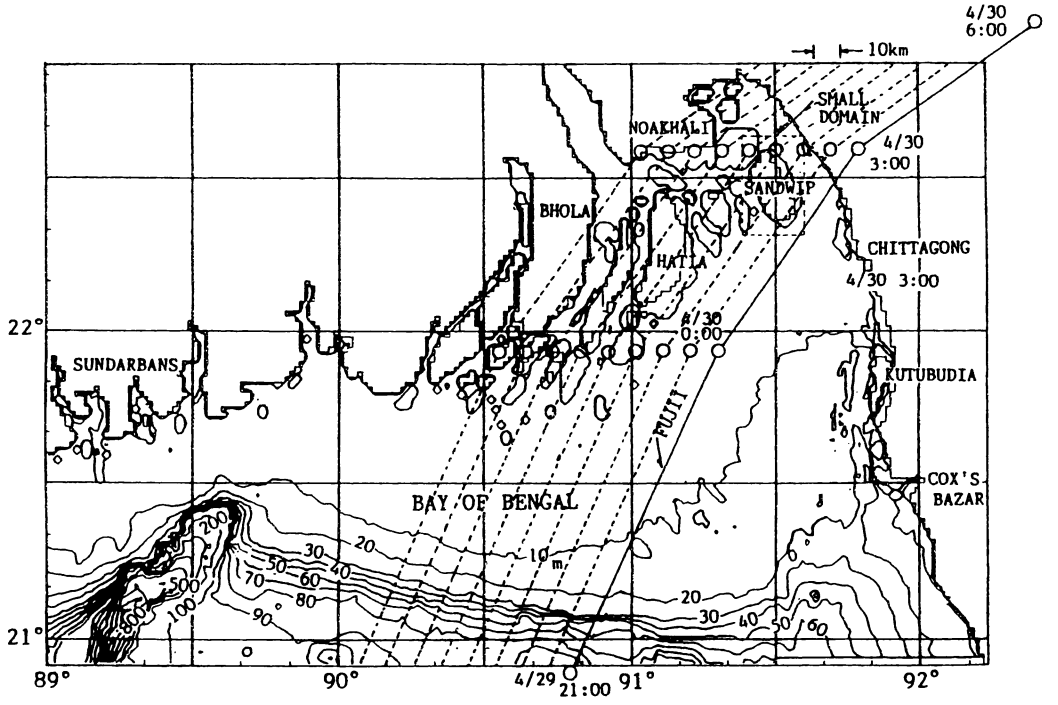

Fig.20 Eight tracking paths of "designed scale cyclone" to predict the most devastating path for Sandwip island.

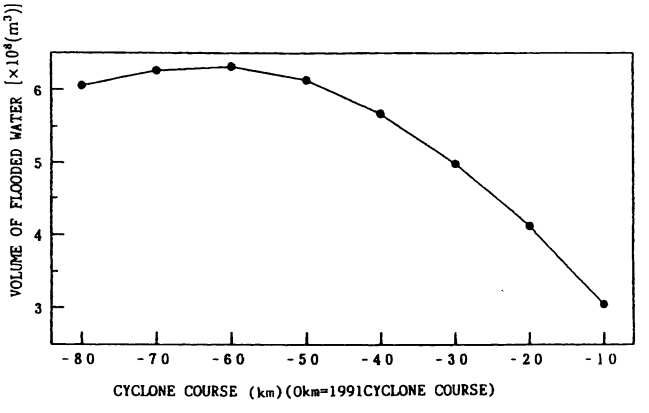

Fig.21 Relation between each cyclone path and the volume of flood water.

the 1991 cyclone path, and investigated in order to find out the most devastating cyclone path for Sandwip island.

We define the "designed cyclone" as a storm whose path generates the maximum volume of flooded water in the island, striking the island during high tide. **Figure 21** shows the relation between each hypothetical cyclone path and the predicted volume of flooded water. From this figure, the cyclone having the same characteristics (the central pressure, the radius of the maximum cyclostrophic wind speed, the difference between the peripheral and central pressures, and moving speed) and taking a path 60 km westward of and parallel to the 1991 cyclone is defined as the "designed cyclone." The reason why the 60 km westward path would be the most devastating for Sandwip island is as follows: As the radius of the maximum cyclostrophic wind speed, r_m used is 60 km, the actual maximum wind speed occurs at $\xi_p = r/r_m = 0.5$, i.e. $r = 0.5 \times 60 = 30$ km, considering the super-gradient wind effect. This means that the maximum wind speed occurs 30 km eastward from the position of the center of the

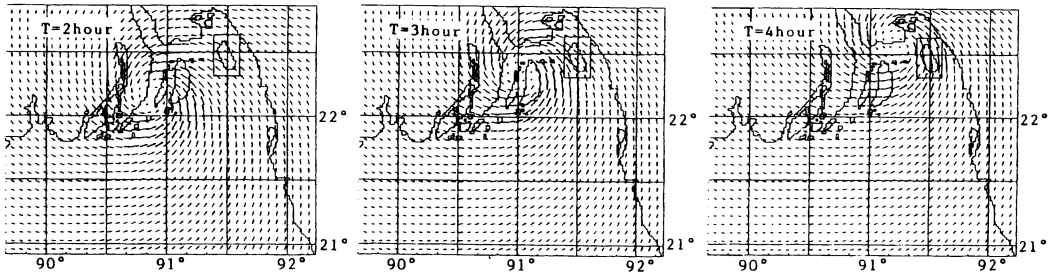

Fig.22 Calculated wind vectors (designed cyclone).

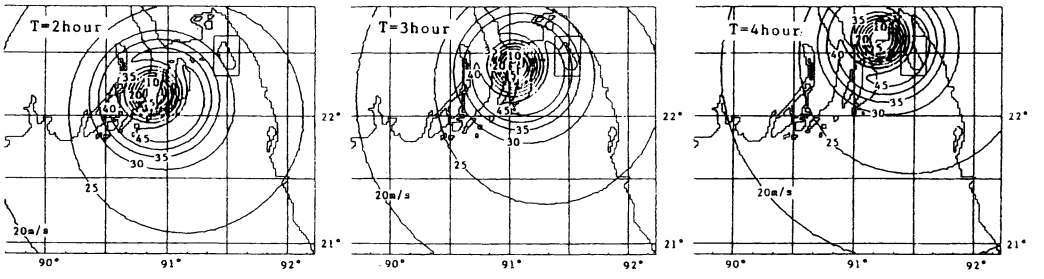

Fig.23 Calculated wind field (designed cyclone).

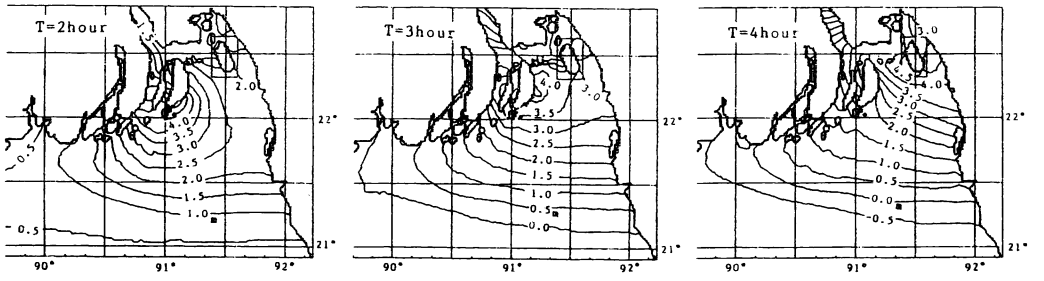

Fig.24 Calculated surge heights (designed cyclone).

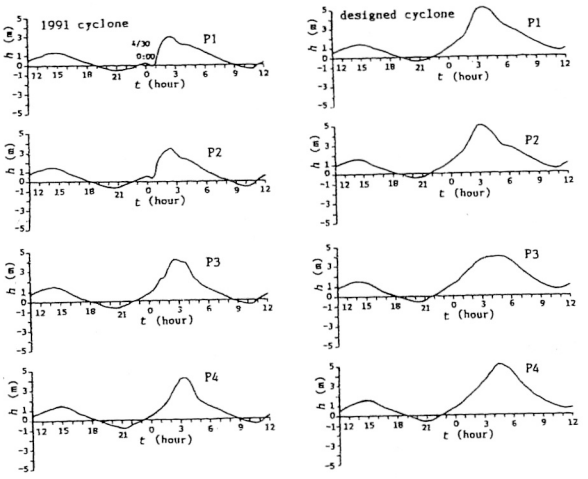

Fig.25 Comparisons of the calculated temporal change of the storm surges by the 1991 cyclone and that by the "designed cyclone" at the points P1～P4.

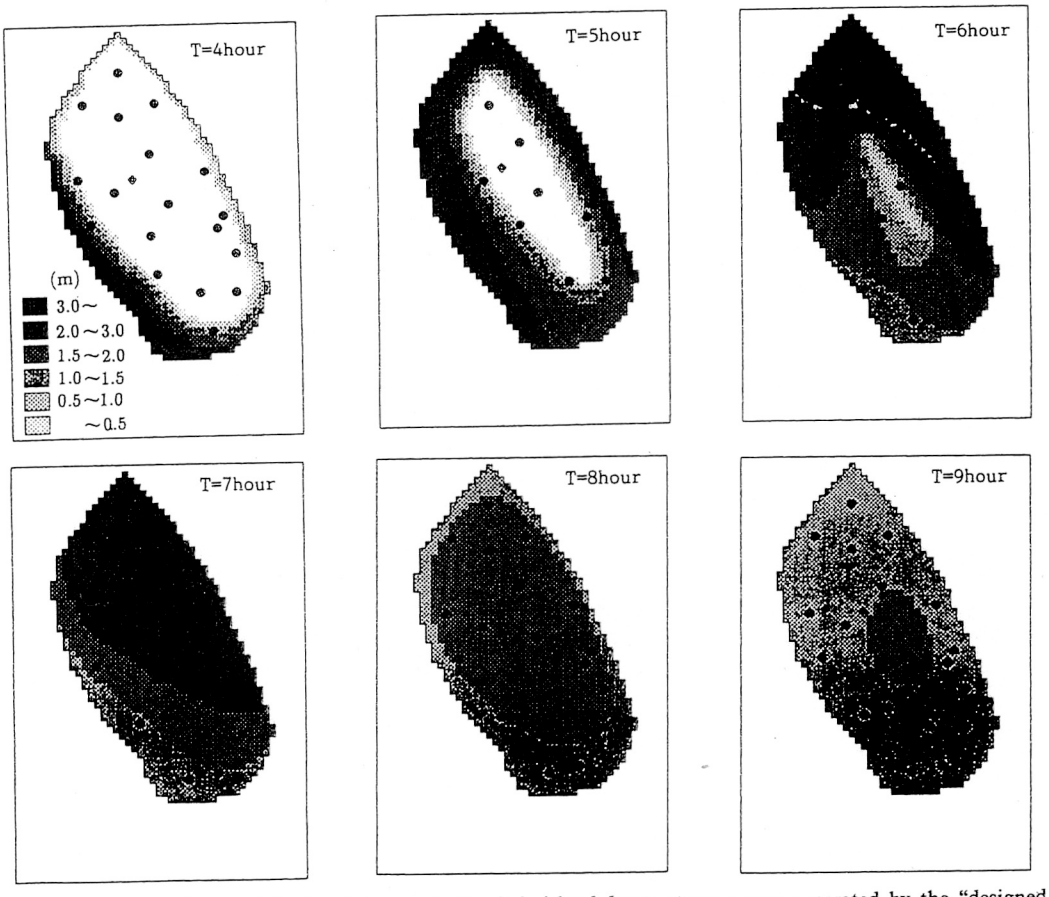

Fig.26 Temporal change of the flooded areas in Sandwip island due to storm surges generated by the "designed cyclone" in the case of no dike breaches.

"designed cyclone" where the west side coast of Sandwip island is situated.

6.2 Storm Surges and Resulting Floods by Designed Cyclone

Figures 22, 23, and **24** show calculated wind vectors, pressure fields, and surge heights for the "designed cyclone", respectively. In these figures, $T = 0$ hour corresponds to 23:00 on 30 April, 1991 in **Fig.10～Fig.12.** It is predicted from **Fig.22** and **Fig.23** that a strong wind would be generated at Sandwip island. This means that the effect of the incremental elevation in the water level caused by wind drift is to be more significant than that caused by the drop in pressure.

Figure 25 compares the calculated temporal change of the storm surges of the 1991 cyclone and that of the "designed cyclone" at points P1～P4. Storm surges due to the "designed cyclone" are greater than those due to the 1991 cyclone at every point. The peak of the storm surges due to the "designed cyclone" would occur at about 3:00 at P1 and P2 where are situated south-west of the island, while occurring at about 5:00 at P3 and P4 in south-east side of the island. Thus, it is understood that the island would be affected by the peak of the storm surges for two hours if attacked by such a devastating cyclone.

Figure 26 shows the predicted temporal changes of the flooded areas due to storm surges which are generated by the "designed cyclone" in the case of no dike breaches. From this figure, the predicted scales of inundation are found to be greater and the speed of flooding to be faster than that of the 1991 cyclone. The heights of cyclone shelters and coastal dikes should be decided by using these calculated results which predict the most devastating possibility.

6.3 Proposal of Countermeasures against Storm Surges

We would like to propose the following countermeasures against storm surges for Sandwip island based on the results of this study:

- Software

  - Acquisition of the accurate information about oncoming cyclones, followed by immediate announcement of storm warnings.
  - Speedy propagation of evacuation orders.
  - Increase of base stations from where evacuation orders would be issued.
  - Education about cyclone and storm surges and their dangerousness to the poorly educated population at both the village and school levels.
  - Education with training for effective evacuation.

- Hardware

  - Construction of many more cyclone shelters at suitable sites.
  - Elevating the evacuation routes.
  - Construction of high and strong coastal dikes.
  - Construction of tide gates at ports.

7. Conclusions

Our method, by which the occurrence of storm surges and the the flooding of protected low-lying areas such as Sandwip island are estimated, has been shown to be very useful for the assessment of countermeasures to be taken against storm surges. First, actual temporal changes in the tide level

produced by the 1991 cyclone were relatively well explained by this simulation method. Moreover, the flooding process in Sandwip island was able to be reproduced by the calculations. Second, it was found that evacuation orders must be issued at least 30 minutes before a dike breach, and the propagation speed of that information must be faster than 5 m/sec, for all evacuees to arrive safely at cyclone shelters. Third, the "designed cyclone" was defined and was created by moving the 1991 cyclone westward and by evaluating the volume of flood water. Finally, we proposed countermeasures against storm surges and the resulting floods.

The dimensions of the coastal dikes, positions of the cyclone shelters and base stations to be constructed, the height of evacuation roads, etc., can be evaluated by the present simulation. Our simulation model and the calculated results can be used as a basis for the design of such countermeasures.

Acknowledgments

We thank Professor Dr. M.M. Hoque and Mr. S.A. Khan who are our counterparts of Bangladesh side (Institute of Flood Control and Drainage Research, Bangladesh University of Engineering and Technology). Some part of this study was financially supported by Grant-in-Aid for General Scientific Research (B) [No.05452376] and (C) [05680368] and Grant-in-Aid for International Scientific Research [04041064] from the Japanese Ministry of Education, Science, Sports and Culture.

References

Choudhury, A.M.: Cyclones in Bangladesh, 24p, 1991.

Flather, A. R.: A Storm Surge Prediction Model for the Northern Bay of Bengal with Application to the Cyclone Disaster in April 1991, Jour. Physical Oceanography, vol.24, pp.172-190, 1994.

Fujii, T. and Y. Mitsuta: Synthesis of a Stochastic Typhoon Model and Simulation of Typhoon Wind, Annuals, Disas. Prev. Res. Inst., Kyoto Univ., No.29B-1, pp.229-239, 1986 (in Japanese).

Inoue, K., H. Nakagawa and K. Shimamoto: Numerical Simulation of Flooding in Cities in the Osaka Bay Area due to Storm Surges, Proc. of 3rd ROC and Japan Joint Seminar on Natural Hazard Mitigation, Taiwan, pp.105-116, 1993.

Institute for Fire Safety and Disaster Preparedness: Comprehensive Bibliography on Regional Disaster Prevention Data, Series on Regional Evacuation, 15p, 1987 (in Japanese).

Iri, M . and T. Kobayashi: The Network Theory, OR Library 12, Nikkagiren, pp.47-52, 1976 (in Japanese).

Committee on Hydraulics, JSCE: Handbook of Hydraulic Engineering, Gihodo, pp.287-288, 1985 (in Japanese).

Katsura, J. *et al.*: Storm Surge and Severe Wind Disasters Caused by the 1991 Cyclone in Bangladesh, Research Report on Natural Disasters, Supported by the Japanese Ministry of Education, Science and Culture (Grant No.03306020), Japanese Group for the Study of Natural Disaster Science, pp.54-82, 1992.

Mitsuta, Y., N. Monji, O. Tsukamoto and H. Asai: Meteorological Study of Typhoon 7705, Annuals, Disas. Prev. Res. Inst., Kyoto Univ., No.21B-1, pp.405-415,1978 (in Japanese).

Nakatsuji, K., S. Watanabe, H. Kurita and N. Yamane: Greenhouse Effects on Storm Surges, A Case Study at Osaka Bay, Japan, Proc. XXV Congress, IAHR, Vol.IV, pp.56-63, 1993.

Nishihara, T.: Evacuation Systems Based on Analyses of Inundation, Doctral Thesis, Kyoto Univ., 192p (in Japanese).

Schwiderski, E.W.: Global Ocean Tides, Part II, The Semidiurnal Principal Lunar Tide (M_2), Atlas of Tidal Charts and Maps, 1979.

Schwiderski, E.W.: Global Ocean Tides, Part III, The Semidiurnal Principal Solar Tide (S_2), Atlas of Tidal Charts and Maps, 1981a.

Schwiderski, E.W.: Global Ocean Tides, Part IV, The Diurnal Luni-Solar Declination Tide (K_1), Atlas of Tidal Charts and Maps, 1981b.

Schwiderski, E.W.: Global Ocean Tides, Part V, The Diurnal Principal Lunar Tide (O_1), Atlas of Tidal

Charts and Maps, 1981c.

Schwiderski, E.W.: Global Ocean Tides, Part VI, The Semidiurnal Elliptical Lunar Tide (N_2), Atlas of Tidal Charts and Maps, 1981d.

Schwiderski, E.W.: Global Ocean Tides, Part IX, The Diurnal Elliptical Lunar Tide (Q_1), Atlas of Tidal Charts and Maps, 1981e.

Schwiderski, E.W.: Global Ocean Tides, Part X, The Fortnightly Lunar Tide (M_f), Atlas of Tidal Charts and Maps, 1982.

Takahashi, T., H. Nakagawa, M. Higashiyama and H. Sawa: Assessment of Evacuation Systems for Water or Mud Floods -A Combined Simulation of Flooding and the Action of Residents-, Jour. Natural Disaster Science, Vol.12, No.2, pp.37-62, 1990.

Yamamoto, R., Y. Mitsuta, N. Monji, O. Tsukamoto and T. Suenobu: Meteorological Study of Typhoon 7709, Annuals, Disas. Prev. Res. Inst., Kyoto Univ., No.21B-1, pp.417-425, 1978 (in Japanese).

(Received June 12, 1995; Revised December 1, 1995)